fibers

MDPI

Article

Structural Evolution of *Gossypium hirsutum* Fibers Grown under Greenhouse and Hydroponic Conditions

Filipe Natalio [1,2,*] and Raquel Maria [3]

[1] Institut für Chemie—Anorganische Chemie, Naturwissenschaftliche Fakultät II—Chemie, Physik und Mathematik, Martin-Luther-Universität Halle-Wittenberg, Kurt-Mothes-Straße 2, 06120 Halle (Saale), Germany
[2] Kimmel Center for Archaeological Science, Weizmann Institute of Science, Rehovot 76100, Israel
[3] Department of Structural Biology, Weizmann Institute of Science, Rehovot 76100, Israel; raquel.isidoro@weizmann.ac.il
* Correspondence: filipe.natalio@weizmann.ac.il; Tel.: +972-8-934-6101

Received: 27 November 2017; Accepted: 19 January 2018; Published: 12 February 2018

Abstract: Cotton is the leading fiber source in the textile industry and one of the world's most important crops. Despite its economic interest, cotton culture exerts an enormous pressure on natural resources (land and water) and has a negative impact on the environment (abuse of pesticides). Thus, alternative cotton growing methods are urged to be implemented. Recently, we have demonstrated that *Gossypium hirsutum* ("Upland" cotton) can be grown in a greenhouse (controlled conditions) and hydroponically. Here we report on the elucidation of the structural changes of the *Gossypium hirsutum* fibers during maturation grown [10, 14, 17, 20, 36 and 51 days post anthesis (dpa)] under a greenhouse and hydroponically, by means of scanning electron microscopy (SEM), Fourier transform infrared spectroscopy with attenuated total reflectance (FT-IR ATR) and thermal gravimetric analysis/differential scanning calorimetry (TGA/DSC). The transition from primary to secondary cell wall growth occurs between 17 and 20 dpa—similarly to the soil-based cultures. However, this new cotton culture offers an advantageous pesticide and soil-free all year-round closed system with efficient water use yielding standardized mature fibers with improved properties (maturity, strength, length, whiteness).

Keywords: cellulose; *Gossypium hirsutum*; structure; development; culture

1. Introduction

Native celluloses have been of prime importance for both scientific interest and industrial applications. However, their structural elucidation has been troublesome [1] due to an intrinsic structural variability prompted by their diversified biological origin [2] and the lack of laboratory-synthesized and/or naturally-occurring standards with a known structure. Today is assumed that cellulose has four different allomorphs (I, II, III and IV) which differ in their unit cell dimensions, chain packing schemes, and hydrogen bonding relationships [3]. Cellulose I is the most abundant form of cellulose in nature and its currently accepted structural model consist of a two-phase model, where a less ordered region and crystalline domains with distinct crystalline forms (I_α and I_β) and variable lateral dimensions coexist in different ratios [4,5]. The ratio between cellulose I_α (triclinic) and cellulose I_β (monoclinic) can be, up to certain extent, correlated to the biological source. I_α is the dominant form found in bacteria and algal cellulose, whereas I_β is the dominant form in higher plants [2,4]. However, due to the structural diversity found within the same species heavily dictated by the environmental conditions, it is not possible to attribute a direct quantification.

Cotton is the leading source of cellulose fibers in the textile industry and one of the world's most important crops [6]. Despite the indisputable economic interest, cotton cultivation is known to exert an enormous pressure on natural resources (land and water) and has a negative impact on the environment (abuse of pesticides). Thus, it seems not only important to implement new forms of sustainable cotton cultivation [7], but also understand and elucidate fiber growth, development and (as far as possible) correlate the different growth stages with a structural/chemical composition [8].

From the physiological point of view, cotton growth starts on the day of anthesis when the epidermal cell of the ovule is fertilized [9,10]. The fiber's cell wall undergoes continuous change in chemical composition [11–13] until it reaches full maturation. The process of cotton growth and development is marked by two sequential cellular events corresponding to primary and secondary cell wall biogenesis. These biologically time-controlled events are generally characterized by fiber elongation and an almost inexistence of cellulose (primary) and the biosynthesis of cellulose and fiber thickening (secondary) [8].

Recently, we have established and implemented forms of sustainable cotton (*Gossypium hirsutum*) growth in opposition to soil-based cultures. We showed that, under these controlled conditions, the mature fiber's structure is consistent with I_β-type of cellulose following the current two-phase model with domains of 4.19 nm surrounded by less ordered regions. From the macroscopic properties (considered the most relevant for potential commercialization purposes), the mature fibers display an improved maturity, strength, length and whiteness [7] in comparison with soil-based cultures. However, this structural characterization was performed at the fiber's mature stage [>51 days post anthesis (dpa)] leaving a structural development information gap over the cotton growth and development, and the impossibility to make a direct comparison with the classic soil-based cultures.

2. Material and Methods

2.1. Cotton Growth

Cotton (*Gossypium hirsutum*) was grown as described elsewhere [7] in a greenhouse under controlled conditions of light, temperature and humidity (minimum 10 klux, 25 °C, 40%). Aseptic seeds were placed in a net pot (5 mm diameter) filled with hydroponic clay pellets. The germination phase was carried out in a propagation box under the conditions mentioned above. Plants displaying first true leaves were transferred to a hydroponic culture system (20 L container *per plant*), aerated by an oxygen pump (air rate 5 L/min) and allow development until full maturity under standard long-day illumination conditions (14/10 h light/dark) and constant watering. 1% (*w*/*v*) fertilizer (Scotts, Peters® Excel, 15+05+15+7CaO+3MgO+TE Cal-Mg Grower, Scotts Deutschland GmbH, Mainz, Germany) was added once per month. On the day of anthesis the flowers were tagged and four developing bolls from four different plants were harvested at 10, 14, 17, 20, 36 and 51 days post anthesis (dpa). The bolls were immediately frozen at −20 °C. After thaw, the pericarp was removed using a sterile scalpel/forceps. The fibers were washed with distilled water three times and dried at room temperature in the absence of tension or straightening. During and after drying the fibers were kept at room temperature and 52% relative humidity (RH) until further characterization.

2.2. Scanning Electron Microscopy (SEM) and Elemental Dispersive X-ray Analysis (EDX)

The air-dried samples were fixed onto a carbon tape (Plano GmbH, Wetzlar, Germany) and its morphology analyzed under a scanning electron microscope (SEM) (JEOL JSM-6710F, JEOL Germany GmbH, Freising, Germany) using 2 kV and 2.5×10^{-6} mbar (chamber vacuum).

2.3. Fourier Transform Infrared Spectroscopy with attenuated total reflectance (FT-IR ATR)

Infrared analysis of air-dried samples was performed using an Agilent Cary 660 spectrometer (Agilent, Waldbronn, Germany) with a DTGS detector fitted with a GladiATR™ (PIKE, Madison, Wisconsin, USA) with a diamond crystal. Spectra were recorded at 4 cm^{-1} resolution and averaging

32 scans. Measurements were performed at room temperature. The background was measured before scanning the samples.

2.4. Thermal Gravimetric Analysis (TGA) and Differential Scanning Calorimetry (DSC)

For simultaneous thermogravimetric (TG) and differential scanning calorimetry (DSC) measurements, the air-dried samples were placed in sealed aluminum crucible and measured in a Netzsch F1 Phoenix (Netzsch-Gerätebau GmbH, Leuna, Germany) with the following conditions: air flow (30 mL/min) with heating rates of 10 K/min up to 800 °C. For the buoyancy correction a baseline was recorded using roughly 40 mg of dry Al_2O_3 and subtracted from the sample measurements. The data was manipulated using OriginLab 8 (v8.0725, OriginLab Corporation, Northampton, MA, USA) and the experiments performed in triplicate. All inflection points from the TGA were determined from the first derivative derivative thermal gravimetric (DTG) transformation of the TGA data (Figure S1). The experiments were performed sequentially on the same day with 52% relative humidity (RH).

3. Results and Discussion

3.1. Macromorphological Characterization of G. hirsutum Fiber Development between 10–51 dpa

A sequence of digital camera images acquired at different time points [10, 14, 17, 20, 36 and 51 post anthesis (dpa)] shows a clear increase of volume as a function of time (Figure 1). From 10 to 17 dpa, the cotton bolls displays a major spherical volume increase, whereas after 17 dpa the growth mainly occurs at opposite directions of the stalks. At 36 dpa, the pericarp starts to be disrupted due to the internal pressure. Between this time point and the 51 dpa, the fully developed cotton fruit is achieved. For further characterization, fibers from all samples were removed with a sterile scalpel, washed with distilled water and air-dried at room temperature in the absence of tension or straightening.

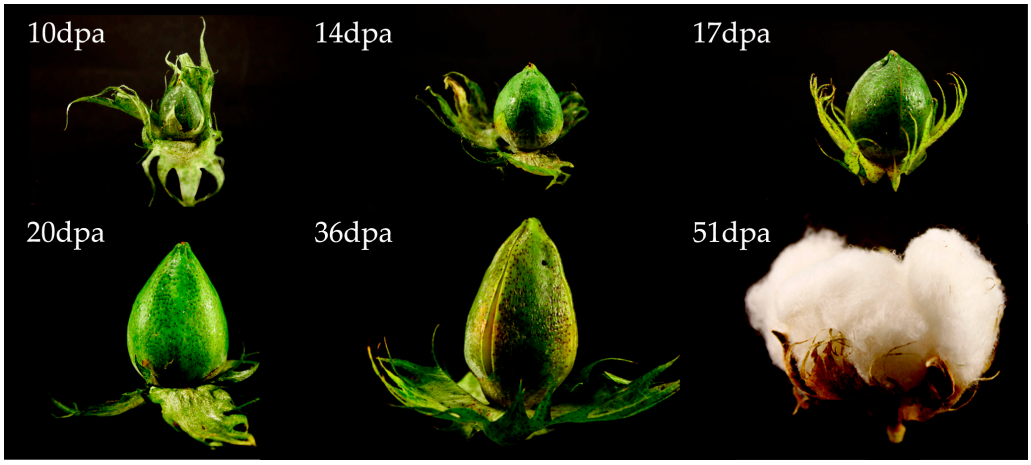

Figure 1. Representative images of different stages of development of *G. hirsutum* cotton (dpa = days post-anthesis) from 10 dpa until it reaches full maturity (51 dpa). During the development, the majority of the fruit volume is found to be between 1–17 dpa. During this period the volume is mainly spherical but after 17 dpa there is a significant morphological modification, i.e, the cotton fruits starts to develop towards the opposite direction of the stalks, yielding a "stretched" morphology until the pericarp full rupture occurs (36–51 dpa).

3.2. Micromorphological Characterization of G. hirsutum Fibers Development between 10–51 dpa

Scanning electron microscopic (SEM) analysis of air-dried samples at 10, 14 and 17 dpa shows stacked fibers with a flattened morphology (average thickness of 141 ± 21, 179 ± 17 and 217 ± 12 nm, respectively), a typical feature for immature fibers (primary cell wall) (Figure 2a upper row) [14].

Fiber stacking can be attributed to a drying effect and the fibers appear always as bundles. At the 17 dpa, the SEM image (Figure 2a lower row) shows fibril -like structures on the surface of the fiber, suggesting the beginning of the secondary cell wall biogenesis. Three days after (20 dpa), a mixture of loose flat and slightly thicker fibers (312 ± 15 nm) is observed, supporting the idea that the primary/secondary cell wall metabolic "switch" occurs around this time frame (Figure 2a lower row). Finally, the fibers at 36 and 51 dpa are well separated and display thicker cell walls with an average thickness of 705 ± 43 nm and 4624 ± 154 nm for 36 and 51 dpa, respectively, and the typical convolutions around the fiber axis [7]. An increased number of convolutions are observed for 51 dpa fibers in comparison with fibers collected at 36 dpa. Interestingly, SEM images of both 17 and 20 dpa samples show the presence of large amounts of spherical features. Elemental chemical analysis (EDX) of these spherical features shows their organic nature with surprisingly high potassium content (9.23 ± 0.31%). However, the function or origin of these organic spheres has not been attributed and/or further explored (Figure S2).

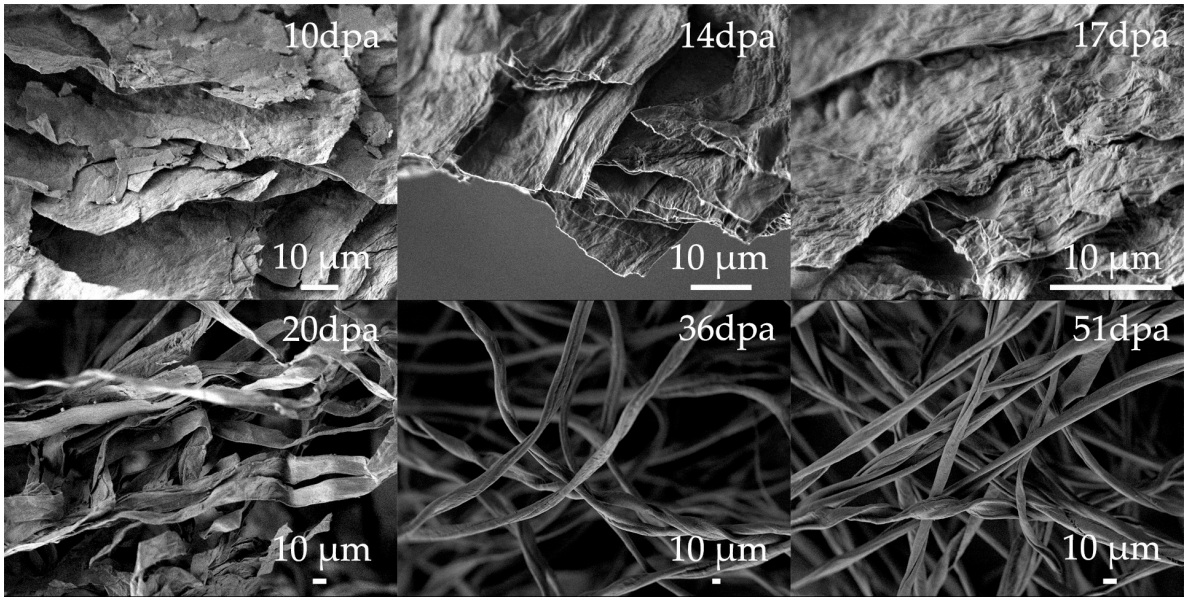

Figure 2. Scanning electron microscopic (SEM) representative images of *G. hirsutum* fibers grown under greenhouse and hydroponic conditions. The fibers were excised at different stages of development (from 10 until 51 dpa where full maturity is reached) without any tension or straightening and air-dried (RT). Until 17 dpa, the fibers display a flat morphology typically attributed to immature fibers. At 20 dpa, a mixture of flat fibers with slightly thicker fibers is found. No convolutions are found at this stage. The process of fiber thickening continues until 51 dpa. This process is accompanied by an increase number of convolutions and attributed to secondary cell wall growth process.

Further complementary structural bulk analyses of fibers collected at different stages of development were performed using FT-IR ATR, TGA and DSC. Prior to carrying out the analysis, all samples were washed in distilled water to remove water soluble molecules (e.g., free glucose), air-dried and further kept under controlled humidity atmosphere (52% RH).

3.3. FT-IR ATR Characterization of G. hirsutum Fibers Development between 10–51 dpa

Figure 3 shows a sequence of representative FT-IR ATR spectra taken from washed and air-dried fibers harvested at different stages of development (10, 14, 17, 20, 36 and 51 dpa). The spectral regions between 3000–3600 cm^{-1} corresponds to stretching vibrations of OH groups derived from both water molecules and intra/inter hydrogen bonding in cellulose [7]. From 10 dpa until 20 dpa, one single broad band is observed whereas at 36 and 51 dpa a double band appears, displaying

higher intensity at 51 dpa. Interestingly, the broad maximum band found between 10 dpa to 20 dpa shifts towards lower wavenumbers, i.e., 3297/3281/3277/3263 cm^{-1} for 10/14/17/20 dpa respectively. Contrary, the maximum band height for the double bands (3277 and 3329 cm^{-1}) found at 36 and 51 dpa remains inalterable in terms of shift and intensity, suggesting a higher level of structural organization. At the current stage, it is not possible to attribute the double band and its significance to cotton fiber structural organization solely on the assumption of an increase of intra- and intermolecular hydrogen bonding [14,15] taking into consideration the contribution of water molecules OH stretching vibrations, their effect on the structural organization of the cellulose chains (hydrogen bonds) and in addition the contribution of homogalacturonans from pectins (OH stretching vibrations) that disappear during the second phase of cell wall synthesis.

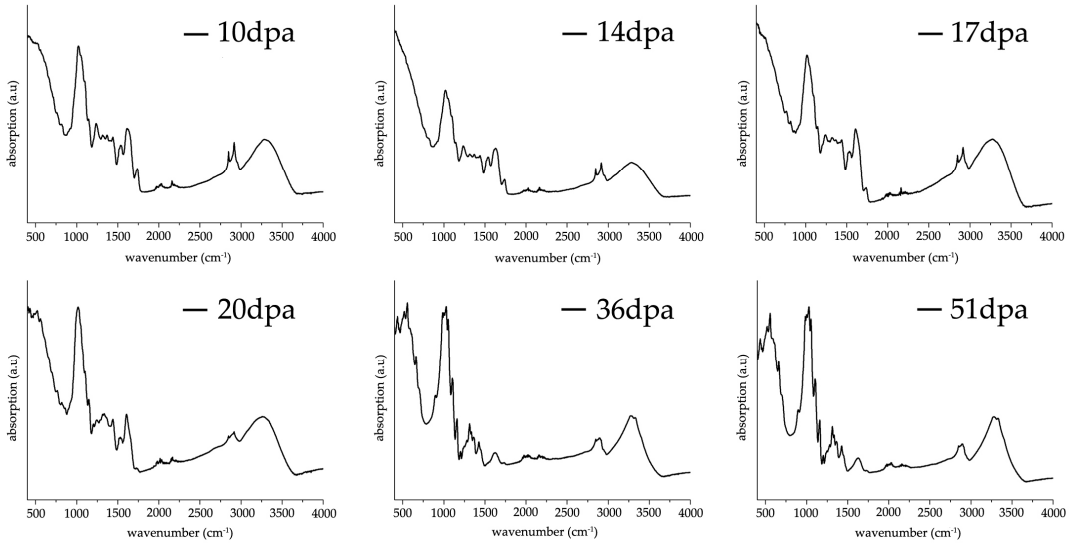

Figure 3. Representative fourier transform infrared spectroscopy with attenuated total reflectance (FT-IR ATR) spectra of raw/washed fibers of *G. hirsutum* harvested at different stages of development (10, 14, 17, 20, 36 and 51 dpa). The fibers were removed without stretching, washed in distilled water prior air-drying at room temperature and kept in a controlled humidity atmosphere (52% RH). Significant spectroscopic differences are observed at 17–20 dpa time threshold indicating that, at this point, the switch from primary to secondary cell wall occurs similarly to the soil-based cultures.

Double sharp bands found at 2848 and 2916 cm^{-1} attributed to CH_2 symmetric stretching are present until 17 dpa, where no band shift is observed. After 17 dpa, both bands intensities decrease to form an undistinguished broad band. Both broadening and band intensity decrease infers a transition from an elongation (primary cell wall synthesis) to a maturation (secondary wall synthesis) process as the ratio between cellulose and non-cellulosic components (e.g., pectins) become higher.

The band located at 1738 cm^{-1} decreases in intensity until 17 dpa without varying its maximum wavenumber. After 17 dpa, this band remains extremely broad and with almost negligible intensity, following a similar trend as found for the bands located at 2848 and 2916 cm^{-1} corresponding to CH_2 symmetric stretching. This band is attributed to C=O stretching of saturated alkyl esters associated to pectins [16], and/or waxes [17] and it is strongly influenced by hydrogen bonds [18]. When 51 dpa *G. hirsutum* fibers grown under the same conditions are treated with NaOH/ ethylenediaminetetraacetic acid/sodium dodecyl sulfate (EDTA/SDS) for 1 h at 80 °C (scouring), this band completely disappears [7] supporting the hypothesis of a hydrophobic nature of the components (waxes or alkylated pectins). Consequently, these findings support the idea that this band can serve to quickly demonstrate the transition between the different stages of cell wall synthesis in *G. hirsutum*.

In the spectral region between 1611 and 1628 cm^{-1} a double broad band at 10 dpa is observed. At 14 dpa, it becomes one single broad band centered at 1630 cm^{-1} displaying a decreased intensity.

Interestingly, between 17 and 20 dpa, this single band sharpens and shifts towards lower wavenumbers (1606 cm^{-1}) but retains its intensity at 17 dpa with a slight increase at 20 dpa. Typically, the vibrations found in this range are associated with the asymmetric stretching of carboxylic acids in the ionic form [18]. At 36 dpa, the band broadens, decreases in intensity and shifts to higher wavenumbers (1623 cm^{-1}). Finally, at 51 dpa an increase in band intensity and shifting to 1630 cm^{-1} is observed in comparison with the 36 dpa band. This wavenumber fluctuation is in opposition to previous findings, where one single band remains at a fixed wavenumber (1633 cm^{-1}) through all developmental stages of *G. hirsutum* L. (soil-based culture) and in which band intensity decrease correlates with the dpa increasing [14,15]. However, this wavenumber variability throughout the different developmental stages, particularly when considering the period between 17 and 20 dpa (1606 cm^{-1}), which represents the metabolic transition between primary and secondary cell wall synthesis, makes the attribution to vibrations corresponding to water molecules (1620 cm^{-1}) and/or amide I (ca. 1620 cm^{-1}) difficult. In fact, this oscillatory process infers a more complex underlying process during this transitory period and provides additional evidence that hydroponic culture impacts the development of *G. hirsutum* when compared with normal soil-based cultures [14,15].

In the region between 1491 and 1568 cm^{-1}, a broad band centered at 1535 cm^{-1} with a shoulder at 1518 cm^{-1} is found at 10 dpa. A band with similar shape but with less intensity is observed at 14 dpa. At 17 and 20 dpa, the bands becomes broader due to the fact that the shoulder observed at 10 and 14 dpa is merged following a similar trend of that found for the bands located at 1606 cm^{-1}, i.e., the 17 dpa band displays a lower intensity than the 20 dpa. At 36 and 51 dpa, no bands in this region are present. The interpretation of this band is straightforward when assuming that the primary and secondary cell wall synthesis transition occurs between 17 and 20 dpa. This vibration is attributed to the NH_2 deformation of amide II, in particular, is a combination of N-H deformation and C-N stretching. Due to fiber thickening the amide II signal becomes obscured and, consequently, it is no longer possible to detect this vibration after the maturation process has evolved (e.g., cellulose shielding).

The vibration found at 1440 cm^{-1} is primarily attributed to CH_2 vibrations (scissoring) of non-cellulosic components. It remains with a fixed maximum wavenumber (1440 cm^{-1}) with a linear intensity decrease until 36 dpa, where the band shifts towards lower wavenumbers (1427 cm^{-1}) with a progressive increase in intensity, attributed to CH_2 symmetric deformation and bending [19], similar to soil-based cultures [14,20].

In addition, the presence of this band at 1427 cm^{-1} has been attributed to an increase in the structural organization of cellulose (e.g., crystalline domains) and used in combination with the vibration correspondent to [β(1-4)glucopyranose] linkage to determine the "crystalline index", later referred to as the "later order index" (LOI) [2,20,21]. A similar trend is found for the double band located at 1313 and 1332 cm^{-1}. Between 10 and 20 dpa, the intensity of this single wide band centered at 1315 cm^{-1} (CH_2 rocking) [19] decreases, whereas after 20 dpa a double band appears with progressively increasing intensity. There seems to be a direct relation between these two vibrations. Apart from the respective CH_2 rocking vibration attributed to this band, there is, however, no significant wavenumber shift (the observed 2 cm^{-1} difference is attributed instrumental error) and no relation to the crystallinity index and/or quantification [15,22]. Interestingly, an intense and broad band found at 1236 cm^{-1} in 10 dpa fibers decreases in intensity until 17 dpa, where a neighboring sharp band located at 1203 cm^{-1} rises until 51 dpa. While the existence of a band at 1245 cm^{-1} has been reported to be present in soil-based cultures and assigned to C=O stretching or NH_2-deformation, it is difficult to assign the same type of vibration to the band located at 1236 cm^{-1} despite the fact that it follows the same trend as found at spectral region between 1611 and 1628 cm^{-1}. On the other side, the band at 1203 cm^{-1} can be, eventually, attributed to C-O in-plane bending or stretching of [β(1-4)glucopyranose] rings and correlated with fiber maturation/development. However this vibration is not fully enough understood to draw conclusions.

At 1145, 1105 and 1052 cm^{-1}, a small shoulder can be identified following a similar behavior as found for soil-based cultures [14,15], i.e., a decrease of intensity until 17 dpa and band shift towards

higher wavenumbers (more pronounced from 1145 cm^{-1} at 10 dpa to 1160 cm^{-1} in 51 dpa) and band sharpening from 36 dpa until 51 dpa. These vibrations are assigned to C-O-C stretching and asymmetrical stretching of non-cellulose molecules and [β(1-4)glucopyranose] rings associated with primary and secondary cell wall development.

A broad asymmetric band centered at 1020 cm^{-1} decreases intensity until 20 dpa. At 36 dpa and 51 dpa, this band displays three peaks at 1029, 1000 and 983 cm^{-1}. Despite the fact that this band is extremely complex for any attempt to attribute any possible vibrations, this is where the major differences between the hydroponic/greenhouse and soil-based *G. hirsutum* cultivars are found. The band typically assigned to the [β(1-4)glucopyranose] linkage is located at 897 cm^{-1}, but only from 36 dpa onwards, indicating that at 36 dpa the development stage is already in the secondary cell wall growth regime.

At 760 cm^{-1} a low-intensity wider band decreases until 17 dpa and disappears afterwards. No band is found at 710 cm^{-1} and thus an assignment to one of the possible cellulose allomorphs using FT-IR ATR is not possible. This is in opposition to the previous assumption that these bands are characteristic of I_β (monoclinic, 710 cm^{-1}) and I_α (triclinic, 750–760 cm^{-1}) and cannot be used for this purpose [23–25]. Using other characterization techniques than FT-IR ATR, the fibers from cotton grown under hydroponic/greenhouse conditions have been classified as cellulose I_β (monoclinic) [7].

In the region below 700 cm^{-1}, four additional bands at 653, 557 (sharp), 518 (shoulder) and 435 cm^{-1} are found, but only for 36 dpa and 51 dpa. Due to their existence only at the later stages of fruit development, these bands might be eventually related with secondary cell wall activity. The FT-IR ATR analysis shows that, despite several marked spectroscopic differences likely attributable to the growing conditions, the transition between primary and secondary cell wall development occurs around the 17–20 dpa similarly to the soil-based cultures.

3.4. TGA/DSC Characterization of G. hirsutum Fibers Development between 10–51 dpa

Thermogravimetric (TGA) and differential scanning calorimetric (DSC) analysis were performed on washed/air-dried fibers kept at 52% RH and retrieved at different time points of fruit development, namely, 10, 14, 17, 20, 36 and 51 dpa. Figure 4a shows an assembly of averaged thermograms obtained for each set of fibers (under air). A cotton cellulose thermogram is, normally, characterized by three weight loss regions ranging between 60–150 °C, 150–250 °C and 250–500 °C, corresponding to water loss and volatile non-cellulosic components (e.g., waxes, fatty acids, esters), and the decomposition of non-cellulosic (e.g., proteins, pectins and hemicellulose) and cellulosic components/char decomposition, respectively. As previously reported, water quantification in non-scoured raw fibers is difficult to attribute due to a masking effect by the coexistence of water molecules and primary cell wall volatile non-cellulosic components [7,17] and even in scoured samples it is almost virtually impossible to distinguish between freezing-bound and non-freezing water fractions.

In region I, the fibers from 10 dpa lose 1.58 ± 0.15% of their initial mass (Figure 4a black line), with a slightly lesser mass loss at 14 dpa (1.02 ± 0.08%) (Figure 4a red line). The percentage mass loss is higher for 17 (Figure 4a light blue line), 20 (Figure 4a dark green line), 36 (Figure 4a pink line) and 51 dpa (Figure 4a light green line) where values of 1.58 ± 0.07%, 3.55 ± 0.04%, 2.42 ± 0.14% and 2.07 ± 0.05% are respectively found. At 150 °C, 10 and 14 dpa shows a percentage mass loss of 7.86 ± 0.6% and 11.04 ± 0.45%, respectively, where 14 dpa represents a certain turning point. From this point on, the percentage mass loss values decreases as the fruit development increases. Values of 10.40 ± 0.08%, 6.62 ± 0.08%, 4.59 ± 0.06% and 3.34 ± 0.05% are found and correspond to 17, 20, 36 and 51 dpa. Interestingly, the thermogram profiles obtained from 10, 14 and 17 dpa show an inflexion point around 100 °C and 20 dpa at 120 °C, whereas the profiles of 36 and 51 dpa show a continuous logarithmic decay from room temperature until 150 °C, indicating a difference in overall composition (first derivative of TGA is found in Figure S1). It seems that 20 dpa is the threshold between primary and secondary cell wall growth supporting the results obtained by FT-IR ATR.

In the region II (150–250 °C), 10 and 20 dpa have a unique thermographic profile and both 14/17 dpa and 36/51 dpa display similar profiles. At 10 dpa, the profile is linearly descending until 212 °C (percentage mass loss of 11.54 ± 0.06%). After this temperature, a pronounced decrease is observed, reaching a percentage mass loss of 17.86 ± 0.08% at 250 °C. For 14 and 17 dpa, inflexion points are observed at 189 and 191 °C with a corresponding percentage mass loss of 20 ± 0.08% and 19.6 ± 0.2%, respectively. From this temperature onwards, both profiles overlap until 250 °C with a corresponding percentage mass loss of 31.40 ± 0.06% and 31.73 ± 0.04% for 14 and 17 dpa. Compared to the percentage mass loss found for 10 dpa at 250 °C, these values are almost two-fold higher. The logarithmic decay-like behavior (i.e., no inflections points) for 20, 36 and 51 dpa continues throughout this temperature range with percentage mass losses of 11.67 ± 0.07%, 6.93 ± 0.07% and 4.49 ± 0.05% at 250 °C, respectively. The behavior found for 14, 17, 20, 36 and 51 dpa thermographic profiles correlates well with the attribution of this region to decomposition of non-cellulosic compounds and the primary/secondary wall switching, i.e., at 14 and 17 dpa the maximum content of non-cellulosic compounds in the fibers is found in opposition to the lower content observed for 20, 36 and 51 dpa.

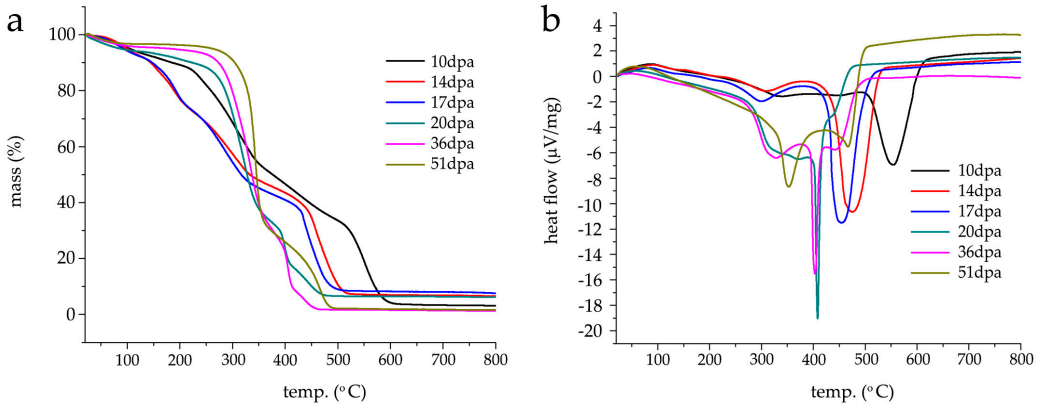

Figure 4. Analysis of raw/washed *G. hirsutum* fibers harvested at different stages of development (10, 14, 17, 20, 36 and 51 dpa). The fibers were removed without stretching, washed in distilled water prior to air-drying at room temperature and kept in controlled humidity atmosphere (52% RH). (**a**) thermogravimetric (TGA) profiles shows the typical three regions, corresponding to water and volatile non-cellulosic (60–150 °C), decomposition of non-cellulosic (150–250 °C), and cellulosic components/char decomposition (250–500 °C); (**b**) Differential scanning calorimetry (DSC) analysis shows a major endothermic band shifting towards lower temperatures as fruit development proceeds. At 51 dpa, this band is centered at 352 °C corresponding to cellulose thermal decomposition and another band centered at 466 °C is assigned to char crystallization processes.

In region three—attributed to the decomposition of cellulosic compounds ranging from 250–500 °C—the profiles differ more significantly between them. The 10 dpa profile shows a smooth inflexion point at 344 °C (44.86 ± 0.2% mass loss) with a linearly decreasing profile until 500 °C where a residual mass loss of 33.61 ± 0.07% assigned to charcoal formation is observed. The 14 and 17 dpa profiles are similar, i.e., they both decrease linearly until approximately 424 °C with major inflexion points appearing at 458 and 435 °C with correspondent percentage mass losses of 69.75 ± 0.45% and 69.95 ± 0.05%. At 500 °C, there is a decrease of mass loss of 89.36 ± 0.25% (14 dpa) and 90.99 ± 0.19% (17 dpa) assigned to the formation of charcoal. These values are three-fold smaller than the one found for the 10 dpa profile suggesting a significantly different chemical composition.

The 20, 36 and 51 dpa profiles show similar behavior between them, i.e., a larger percentage mass loss is clearly observed in the temperature range between 250–375 °C and a smaller percentage mass loss beyond 400 °C and three plateaus. At 20 dpa, two major inflexion points are found at 324 and 399 °C with correspondent percentage mass losses of 47.12 ± 0.25% and 75.07 ± 0.74%. At 500 °C, the mass loss is of 93.4 ± 0.5%. Interestingly, the 36 dpa profile is very similar to that of 20 dpa.

However, the two major inflexion points are found at 334 °C (9 °C higher than 20 dpa) and 405 °C (6 °C higher than 20 dpa) with a correspondent percentage mass loss of 47.3 ± 0.47% and 82.96 ± 0.45%. At 500 °C, the mass loss is of 98.32 ± 0.34%. The difference in these values suggests that the fibers are in a transitory chemical composition. The 51 dpa fibers show one major inflexion point at 343 °C and one less pronounced inflexion point at 466 °C and a mass loss of 43.4 ± 0.55% and 90.9 ± 0.37%, respectively. At 500 °C, the mass loss is of 97.98 ± 1.54%. In the cases of 36 and 51 dpa, the values of residual mass are far smaller than the values found for the other fibers at different development stages leading to the conclusion that at these (later) stage fibers are composed, in the majority, by cellulosic compounds. Despite the FT-IR ATR growth profile similarity, it is in thermogravimetric profiles from hydroponic/greenhouse fibers collected at different stages that the differences with soil-based cultures are more pronounced [14,15,17]. The thermogravimetric analysis shows that the fibers at different stages of development have different chemical compositions when grown under hydroponic/greenhouse conditions.

To confirm the assumption laid by thermogravimetric analysis and the FT-IR ATR dataset, the DSC analysis of the raw/washed fibers collected at different time points was also carried out, namely, 10 (Figure 4b black line), 14 (Figure 4b red line), 17 (Figure 4b blue line), 20 (Figure 4b dark green line), 36 (Figure 4b pink line) and 51 dpa (Figure 4b light green). Despite the different profiles, an underlying trend is observed, i.e., as fruit development advances the major exothermic event appears at lower temperatures similarly to soil-based cultures [17]. Despite this similar trend, the profiles for the fibers grown under hydroponic/greenhouse cultures differ significantly from soil-based cultures, reinforcing the idea that hydroponic/greenhouse conditions significantly impact the cotton development [17]. It is worth noting that the DSC analysis was carried out in washed/raw fibers. It is known that the washing step removes substances and reduces the thermogram complexity by displaying fewer thermal transitions in the lower temperature region (room temperature −150 °C). However, the differences observed for the profiles obtained by hydroponic/greenhouse-grown fibers and soil-based fibers are pronouncedly different and cannot be attributed to this "simplifying" step. The thermogram profiles for 10, 14 and 17 dpa show major symmetric endothermic bands at 553, 474 and 454 °C assigned to the crystallization temperature (T_c), a smaller endothermic band at 339, 309 and 300 °C and an exothermic band at 86 and 84 °C, respectively. These higher temperature values overlap with the major percentage mass losses observed on the thermogravimetric analysis (Figure 4a). Interestingly, the thermogram profile found at 20 and 36 dpa differs significantly from all the other previous profiles. It shows a very sharp symmetric band with its lowest point at 408 °C (20 dpa) and 403 °C (36 dpa) assigned to the crystallization temperature (T_c), respectively (Figure 4b dark green and pink). However, this sharp band found at 36 dpa is combined with two other endothermic wider and less intense bands centered at 327 °C and 441 °C. According to the thermogravimetric analysis (see Table 1 for summary), the highest percentage mass loss found in the 36 dpa fibers coincides with the temperature corresponding to this wider and less intense endothermic band located at 327 and can be assigned to cellulose thermal decomposition [17]. The major symmetric and sharp endothermic band is, in turn, assigned to charcoal formation. In 20 dpa and 36 dpa profiles, exothermic bands are found at 56 and 47 °C, respectively and eventually attributed to waxes [17]. At 51 dpa, the DSC profile shows two pronounced endothermic bands (Figure 4b light green line), one larger and symmetric band centered at 353 °C and the second smaller, asymmetric and centered at 466 °C. The band located at 353 °C corresponds to the crystallization temperature (T_c) and assigned to cellulose thermal decomposition infers the complete absence of primary cell wall with a well-defined chemical composition. As in the previous profiles, a small exothermic band is observed at 59 °C. A summary of the thermal behavior of *Gossypium hirsutum* fibers is presented in Table 1.

Table 1. Summary of the thermal behavior of *Gossypium hirsutum* fibers harvested at different stages of development (10, 14, 17, 20, 36 and 51 dpa).

Thermal Gravimetric Analysis Summary (% Mass Loss)								**Differential Scanning Calorimetry Summary (°C)**		
	region I (60–150 °C)		region II (150–250 °C)		region III (250–500 °C)			exothermic	endothermic	
dpa	60 °C	150 °C	(temp. of inflection point)	250 °C	(temp. of first inflection point)	(temp. of second inflection point)	500 °C		small	sym, major, T_C
10	1.58 ± 0.15	7.86 ± 0.6	11.54 ± 0.06 (212 °C)	17.86 ± 0.08	44.86 ± 0.2 (344 °C)	-	33.61 ± 0.07	86	339	553
14	1.02 ± 0.08	11.04 ± 0.45	20 ± 0.08 (189 °C)	31.40 ± 0.06	69.75 ± 0.45 (458 °C)	-	89.36 ± 0.25	91	309	474
17	1.58 ± 0.07	10.40 ± 0.08	19.6 ± 0.05 (191 °C)	31.73 ± 0.04	69.95 ± 0.05 (435 °C)	-	90.99 ± 0.19	84	300	454
20	3.55 ± 0.04	6.62 ± 0.08	-	11.67 ± 0.07	47.12 ± 0.25 (324 °C)	75.07 ± 0.74 (399 °C)	93.4 ± 0.5	56	-	408
36	2.42 ± 0.14	4.59 ± 0.06	-	6.93 ± 0.07	47.3 ± 0.47 (334 °C)	82.96 ± 0.45 (405 °C)	98.32 ± 0.34	47	327/441	403
51	2.07 ± 0.05	3.34 ± 0.05	-	4.49 ± 0.05	43.4 ± 0.55 (343 °C)	90.9 ± 0.37 (466 °C)	97.98 ± 1.54	59	466	353

4. Conclusions

Cotton's economic importance is indisputable. Current worldwide agricultural practices of cotton cultivation seem unsustainable in the long term and, thus, alternative and sustainable solutions are urged to be implemented in parallel. Here we have reported a follow-up study on the structural characterization of *G. hirsutum* fibers harvested at different stages of development (10, 14, 17, 20, 36 and 51 dpa) grown under controlled conditions and hydroponically. This study demonstrates that the cotton growth and development under hydroponic/greenhouse cultures follows equally a two-stage process with a biochemical and cellular "switch" between 17 and 21 dpa, similar to that found in soil-based cultures. Despite the fact that the cotton growth and development is not accelerated under hydroponic/greenhouse conditions, this culture method offers the advantage of producing standardized (high) fiber quality—an important trait for large-scale applications/uses—and the possibility to grow cotton all year round with a reduced (negative) environmental impact. Moreover, understanding the developmental timeline of this new cotton cultivation method opens the doors for the implementation of the biofabrication concept.

Supplementary Materials: The following are available online at http://www.mdpi.com/2079-6439/6/1/11/s1. Figure S1: First derivative of the thermal profiles of raw/washed G. hirsutum fibers harvested at different stages of development (10, 14, 17, 20, 36 and 51 dpa) obtained from Figure. 4a. Figure S2: Representative scanning electron microscope images of fibers taken at (a) 17dpa and (b) 20 dpa (days post-anthesis) showing a spherical features; (c) higher magnification of spherical features. The electron accumulation suggests an organic nature. The square represents the area where the chemical analysis was carried out; (d) representative spectra obtained for the chemical elemental analysis of the spherical features showing the presence of high concentration of potassium and confirming the organic nature of these features.

Acknowledgments: This work was financially supported by the Forschungsschwerpunkt Nano-strukturierte Materialien (NWG IV: Bioanorganische Chemie) Ministerium für Wissenschaft und Wirtschaft des Landes Sachsen-Anhalt, Germany. We thank *Roberto Köferstein* (Institute for Inorganic Chemistry, Martin Luther University Halle-Wittenberg, Halle (Saale), Germany) for his help with the TGA/DSC measurements.

Author Contributions: Raquel Maria and Filipe Natalio designed the research. Raquel Maria and Filipe Natalio performed the experiments. Both authors analyzed data. Filipe Natalio wrote the manuscript. Both authors approved the manuscript.

Conflicts of Interest: The authors declare no conflict of interest.

References

1. Atalla, R.H.; VanderHart, D.L. The role of solid state ^{13}C NMR spectroscopy in studies of the nature of native celluloses. *Solid State Nucl. Magn. Reson.* **1999**, *15*, 1–19. [CrossRef]
2. Krässig, H.A. *Cellulose Structure, Accessibility and Reactivity*, 2nd ed.; Gordon and Breach Science Publishers: Yverdon, Switzerland, 1993.
3. Weimer, P.J.; French, A.D.; Calamari, T.A. Differential fermentation of cellulose allomorphs by ruminal cellulolytic bacteria. *Appl. Environ. Microbiol.* **1991**, *57*, 3101–3106. [PubMed]
4. Atalla, R.H.; Vanderhart, D.L. Native cellulose: A composite of two distinct crystalline forms. *Science* **1984**, *223*, 283–285. [CrossRef] [PubMed]
5. Park, S.; Baker, J.O.; Himmel, M.E.; Parilla, P.A.; Johnson, D.K. Research cellulose crystallinity index: Measurement techniques and their impact on interpreting cellulase performance. *Biotechnol. Biofuels* **2010**, *3*, 1–5. [CrossRef] [PubMed]
6. John, M.E.; Stewart, J.M. Genes for jeans: Biotechnological advances in cotton. *Trends Biotechnol.* **1992**, *10*, 165–170. [CrossRef]
7. Natalio, F.; Tahir, M.N.; Friedrich, N.; Köck, M.; Fritz-Popovski, G.; Paris, O.; Paschke, R. Structural analysis of *Gossypium hirsutum* fibers grown under greenhouse and hydroponic conditions. *J. Struct. Biol.* **2016**, *194*, 292–302. [CrossRef] [PubMed]
8. Delmer, D.P. Cellulose biosynthesis: Exciting times for a difficult field of study. *Annu. Rev. Plant Biol.* **1999**, *50*, 245–276. [CrossRef] [PubMed]
9. Stewart McD, J. Fiber initiation on the cotton ovule (*Gossypium hirsutum*). *Am. J. Bot.* **1975**, *62*, 723–730. [CrossRef]

10. Anderson, D.B.; Kerr, T. Growth and structure of cotton fiber. *Ind. Eng. Chem. Res.* **1938**, *30*, 48–54. [CrossRef]
11. Meinert, M.C.; Delmer, D.P. Changes in biochemical composition of the cell wall of the cotton fiber during development. *Plant Physiol.* **1977**, *59*, 1088–1097. [CrossRef] [PubMed]
12. Maltby, D.; Carpita, N.C.; Montezinos, D.; Kulow, C.; Delmer, D.P. β-1,3-Glucan in Developing Cotton Fibers: Structure, Localization, and Relationship of Synthesis to That of Secondary Wall Cellulose. *Plant Physiol.* **1979**, *63*, 1158–1164. [CrossRef] [PubMed]
13. Huwyler, H.R.; Franz, G.; Meier, H. Changes in the composition of cotton fiber Cell walls during development. *Planta* **1979**, *146*, 635–642. [CrossRef] [PubMed]
14. Abidi, N.; Hequet, E.; Cabrales, L.; Gannaway, J.; Wilkins, T.; Wells, L.W. Evaluating cell wall structure and composition of developing cotton fibers using Fourier transform infrared spectroscopy and thermogravimetric analysis. *J. Appl. Poly. Sci.* **2008**, *107*, 476–486. [CrossRef]
15. Abidi, N.; Cabrales, L.; Haigler, C.H. Changes in the cell wall and cellulose content of developing cotton fibers investigated by FTIR spectroscopy. *Carbohydr. Polym.* **2014**, *100*, 9–16. [CrossRef] [PubMed]
16. Sene, C.F.; McCann, M.C.; Wilson, R.H.; Grinter, R. Fourier-transform Raman and Fourier-transform infrared spectroscopy (an investigation of five higher plant cell walls and their components). *Plant Physiol.* **1994**, *106*, 1623–1631. [CrossRef] [PubMed]
17. Hartzell-Lawson, M.M.; Hsieh, Y.L. Characterizing the noncellulosics in developing cotton fibers. *Text. Res. J.* **2000**, *70*, 810–819. [CrossRef]
18. Chen, L.; Wilson, R.H.; McCann, M.C. Infrared microspectroscopy of hydrated biological systems: Design and construction of a new cell with atmospheric control for the study of plant cell walls. *J. Microsc.* **1997**, *188*, 62–71. [CrossRef]
19. Liang, C.Y.; Marchessault, R.H. Infrared spectra of crystalline polysaccharides. II. Native celluloses in the region from 640 to 1700 cm^{-1}. *J. Polym. Sci.* **1959**, *39*, 269–278. [CrossRef]
20. Hsieh, Y.L.; Hu, X.P.; Nguyen, A. Strength and crystalline structure of developing Acala cotton. *Text. Res. J.* **1997**, *67*, 529–536. [CrossRef]
21. O'Connor, R.T.; DuPre, E.F.; Mitchum, D. Applications of infrared absorption spectroscopy to investigations of cotton and modified cottons Part I: Physical and crystalline modifications and oxidation. *Text. Res. J.* **1958**, *28*, 382–392. [CrossRef]
22. Schwanninger, M.; Rodrigues, J.C.; Pereira, H.; Hinterstoisser, B. Effects of short-time vibratory ball milling on the shape of FT-IR spectra of wood and cellulose. *Vib. Spectrosc.* **2004**, *36*, 23–40. [CrossRef]
23. Imai, T.; Sugiyama, J. Nanodomains of I_α and I_β cellulose in algal microfibrils. *Macromolecules* **1998**, *31*, 6275–6279. [CrossRef]
24. Sassi, J.F.; Tekely, P.; Chanzy, H. Relative susceptibility of Iα and Iβ phases of cellulose towards acetylation. *Cellulose* **2000**, *7*, 119–132. [CrossRef]
25. Akerholm, M.; Salmen, L. Dynamic FTIR spectroscopy for carbohydrate analyses of wood pulp. *J. Pulp. Pap. Sci.* **2002**, *28*, 245–249.